Title

Optimized pulses for Raman excitation through the continuum: Verification using the multiconfigurational time-dependent Hartree-Fock method

Journal

Physical Review A, 96(1)

ISSN

2469-9926

Authors

Greenman, Loren
Whaley, K Birgitta
Haxton, Daniel J
et al.

Publication Date

2017-07-01

DOI

10.1103/physreva.96.013411

Peer reviewed

Optimized pulses for Raman excitation through the continuum: verification using multi-configurational time-dependent Hartree-Fock

Loren Greenman,[1,2] K. Birgitta Whaley,[2,1] Daniel J. Haxton,[1] and C. William McCurdy[3,4,*]

[1] *Chemical Sciences, Lawrence Berkeley National Laboratory, Berkeley, CA 94720, USA*
[2] *Department of Chemistry and Kenneth S. Pitzer Center for Theoretical Chemistry, University of California, Berkeley, CA 94720, USA*
[3] *Chemical Sciences and Ultrafast X-ray Science Laboratory, Lawrence Berkeley National Laboratory, Berkeley, CA 94720, USA*
[4] *Department of Chemistry, University of California, Davis, California 95616, USA*

(Dated: September 16, 2016)

We have verified a mechanism for Raman excitation of atoms through continuum levels previously obtained by quantum optimal control using the multi-configurational time-dependent Hartree-Fock (MCTDHF) method. This mechanism, which was obtained at the time-dependent configuration interaction singles (TDCIS) level of theory, involves sequentially exciting an atom from the ground state to an intermediate core-hole state using a long pump pulse, and then transferring this population to the target Raman state with a shorter Stokes pulse. This process represents the first step in a multidimensional x-ray spectroscopy scheme that will provide a local probe of valence electronic correlations. Although at the optimal pulse intensities at the TDCIS level of theory the MCTDHF method predicts multiple ionization of the atom, at slightly lower intensities (reduced by a factor of about 4) the TDCIS mechanism is shown to hold qualitatively. Quantitatively, the MCTDHF populations are reduced from the TDCIS calculations by a factor of 4.

I. INTRODUCTION

Whereas linear spectroscopy directly measures the energies of states via the first-order response function, multidimensional spectroscopy measures couplings between states using higher-order response functions. Multidimensional spectroscopies are currently used to measure couplings in the regimes of radiowaves (NMR) [1–3], infrared (vibrational) [4, 5], and UV-Vis (photon echo) [6–10]. An x-ray analog of such spectroscopies could be used to measure couplings between localized core-hole excitations [11, 12]. Such couplings are due to valence electron interactions, and therefore x-ray multidimensional spectroscopy provides a local probe of valence excitations. However, complications arise due to the high energy of x-ray pulses, which can ionize samples or cause other unwanted processes to occur.

We are developing the ability to coherently control x-rays and shape laser pulses to avoid ionization and other unwanted processes. Two of the authors (LG and KBW) have recently obtained pulses that perform the first crucial step of a multidimensional x-ray scheme while avoiding ionization [13]. This was accomplished by combining Krotov's optimal control method [14–19] with time-dependent configuration interaction singles (TDCIS) electronic dynamics including the ionization continuum [20, 21]. The TDCIS method is a good choice for optimal control calculations, it is computationally cheap and captures low-order electron correlation by including all singly excited electronic configurations. However, TDCIS ignores multiply excited pathways, and so the reliability of the optimal pulses in an experimental setting is unclear. In this work, we use the multiconfigurational time-dependent Hartree-Fock (MCTDHF) [22, 23] method to verify that the pulses we found work after including higher-order electron correlation. MCTDHF includes all excitation pathways within a subset of orbitals, which are time-dependent (unlike TDCIS, which uses time-independent orbitals).

Previously, the authors CWM and DJH used MCTDHF to perform Raman excitation of Li [24] and NO [25]. In both of these references, as well as Ref. [13] and this work, the first step in a multidimensional scheme is attempted, and the intermediate state of the Raman process is a resonance state above the level of the electronic ionization continuum. Additionally, all of these works have found adiabatic mechanisms such as stimulated Raman adiabatic passage (STIRAP) [26] to be ineffective at the energy and timescales of interest. In Refs. [24] and [25], the large amount of background ionization due to absorption of the x-ray pulses by spectator orbitals was avoided by choosing inner core levels to address. The high-energy x-rays that address these levels have a much lower cross section for absorption by spectator orbitals. In the case of Ref. [24], Li has no occupied p-orbitals to contribute to background ionization. In contrast, in Ref. [13], optimal control theory was used to find pulses that minimize background ionization but penalizes distance from some guess pulse. A mechanism was therefore found to excite a Raman excitation using pulses with lower energies, although a smaller fraction of the final wavefunction is in the Raman state. Furthermore, the coherent excitation of the Raman state was considered in Ref. [13], and pulses were obtained that excite the Raman state with a fixed phase relative to the ground state.

*Electronic address: cwmccurdy@lbl.gov

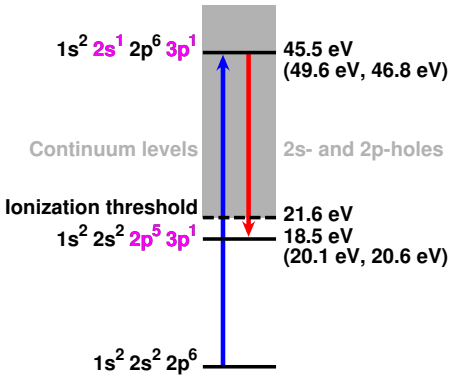

FIG. 1: (Color online) The target Raman process is pictured. The pump (red) pulse excites the intermediate (2s-3p) state, then the Stokes (blue) pulse transfers the population to the desired (2p-3p) state. The experimental energy levels are given along with the TDCIS (from diagonalization) and MCTDHF (determined as in Fig. 3) energy levels in parentheses.

The optimizations performed with TDCIS uncovered specific pulses and also a more general mechanism for generating pulse sequences that perform x-ray Raman while avoiding ionization [13]. In this sequential mechanism, a long pump pulse is first used to selectively excite population from the ground state to the intermediate state, and then a shorter Stokes pulse is used to transfer population from the intermediate state to the desired state. The long pump pulse selects the transition to the intermediate state, which is located close in energy to a dense number of continuum states, and avoids background transitions to those states. If a specific phase is desired between the Raman state and ground state, it can be imprinted via the carrier envelope phase of the pump pulse (see Ref. [13]). The length of the Stokes pulse is somewhat flexible, but it must be short enough to overcome autoionization from the intermediate state. The ideal placement of the Stokes pulse is near the peak of the intermediate state population, which TDCIS predicts to be slightly before the pump pulse maximum for a pump pulse on the order of 50 fs.

As discussed in Ref. [13], we use Ne as an example because of its accessibility to tabletop experiments and free electron lasers such as FERMI@Elettra [27]. The levels we are targeting are shown in Fig. 1. The intermediate state is the 2s-3p state of Ne, which lies above the ionization threshold. The target state is the 2p-3p valence excitation.

We find that up to a factor lower than an order of magnitude, electron correlation effects do not destroy the efficacy of the optimal pulses. This is true only up to a certain intensity, however, above which multiple ionization pathways make TDCIS unreliable.

II. THEORY

Both the time-dependent configuration interaction singles (TDCIS) [20, 21] method and the multiconfigurational time-dependent Hartree-Fock (MCTDHF) [22, 23] method choose a reference configuration ($|\Phi_0\rangle$) that is an antisymmetrized product of N_e single-particle orbitals,

$$|\Phi_0\rangle = |\phi_1\phi_2\dots\phi_{N_e}\rangle. \tag{1}$$

Both methods describe the many-electron wavefunction using this reference and configurations obtained by exciting particles from the reference,

$$|\Phi_i^a\rangle = \hat{a}_a^\dagger\hat{a}_i|\Phi_0\rangle \tag{2}$$
$$|\Phi_{i,j}^{a,b}\rangle = \hat{a}_a^\dagger\hat{a}_b^\dagger\hat{a}_j\hat{a}_i|\Phi_0\rangle,\dots, \tag{3}$$

where i,j denote orbitals occupied in the reference and a,b denote unoccupied orbitals and $\hat{a}$ and $\hat{a}^\dagger$ denote annihilation and creation operators, respectively.

In the configuration interaction singles (CIS) method, the reference (Eq. (1)) and *all* singly-excited configurations (Eq. (2)) are included (up to a very high energy cutoff),

$$|\Psi(t)\rangle = \alpha_0(t)|\Phi_0\rangle + \sum_{i,a}\alpha_i^a(t)|\Phi_i^a\rangle. \tag{4}$$

In this configuration space, dynamic electron correlation between singly-excited configurations is taken into account. Due to Brillouin's theorem, there is no mixing between the reference configuration and excited configurations due to Coulomb interactions. CIS, therefore, provides a first-order description of excited states dominated by single-particle configurations. Excitations that involve multiple occupied orbitals are not qualitatively well-described by CIS. Time-dependent CIS (TDCIS) uses time-dependent coefficients on the CIS configurations to describe the time-evolving wavefunction. The orbitals ϕ_i remain time-*independent*, in contrast to the MCTDHF method. TDCIS can not describe multiple ionization pathways.

The MCTDHF method [22, 23, 28–32], as implemented in Refs. [22, 23], uses a smaller subset of N_o orbitals, $\{\phi_{sub}\} = \{\phi_1,\dots,\phi_{N_o}\}$, but includes all configurations in this subset. This means that multiply ionized pathways can be described. The coefficients on each configuration and the shape of the orbitals that define the reference and excited configurations are both time-dependent.

$$\begin{aligned}|\Psi(t)\rangle &= \alpha_0(t)|\Phi_0(t)\rangle + \sum_{i,a\in\{\phi_{sub}\}}\alpha_i^a(t)|\Phi_i^a(t)\rangle \\ &+ \sum_{i,j,a,b\in\{\phi_{sub}\}}\alpha_{i,j}^{a,b}(t)|\Phi_{i,j}^{a,b}(t)\rangle + \dots\end{aligned} \tag{5}$$

It should be noted that MCTDHF using restricted configuration spaces is also being developed [33]. MCTDHF mainly captures static (nondynamic) correlation, in other

words the contribution from configurations that at zeroth order define the wavefunction. For instance, double ionization from the core is described at zeroth order using a doubly excited configuration, and TDCIS can not describe this. Throwing away orbitals, however, leads to a greater amount of dynamic correlation being left out, but the time-dependent nature of the orbitals could possibly reintroduce some dynamic correlation back into the calculation. Furthermore, dynamic correlation tends to lead to quantitative, and not qualitative, corrections to the wavefunction.

One further difference between the TDCIS method used in Ref. [13] and the MCTDHF method is the description of the ionization continuum. The TDCIS method uses a complex absorbing potential (CAP) [20, 34, 35], an imaginary quadratic potential that is turned on after a cutoff radius. CAPs can be tuned to capture a small number of resonance energies correctly, but they can also perturb the bound states and continuum states outside the region for which they're tuned. MCTDHF instead uses exterior complex scaling (ECS) [36, 37], in which the spatial coordinates are scaled into the complex plane by an angle θ. ECS has been shown to effectively treat continuum levels [37], and it does not perturb the bound states.

Comparing MCTDHF and TDCIS propagations using the optimal pulses determined with Krotov's method in Ref. [13], we will gain a view of the time-dependent processes in the x-ray Raman excitation of atoms.

The MCTDHF calculations shown in this work were obtained using a space of 9 orbitals, the $1s$, $2s$, $2p$, $3s$, and $3p$ orbitals of Ne. We used a spatial grid of six 4.7 Å elements, each with 19 grid points, with an angular momentum maximum of $L = 4$ and $M = 2$. Bill and/or Dan: I'm not sure what the proper notation would be for the angular grid. The last element was complex scaled using an angle of 0.4 radians.

III. RESULTS AND DISCUSSION

The mechanism for x-ray Raman excitation of atoms while avoiding ionization is as follows: first, a long pump pulse is used to selectively excite the intermediate state (the 2s-3p state of Ne), followed by a shorter Stokes pulse that beats the autoionization of the intermediate state and transfers the population to the desired state (in Ne, the 2p-3p state). This mechanism was uncovered using TDCIS and optimal control theory, and it was used to develop experimentally realizeable pulses. A 50 fs, 71 μJ pump pulse and 0.5 fs, 0.71 μJ Stokes pulse represent one choice of pulses, and there were other options, especially regarding the length of the Stokes pulse. The peak intensity of the pump pulse was 6.1×10^{14} W/cm^2.

Since MCTDHF and TDCIS have different descriptions of the electron correlation, the transition frequencies at each level of theory will be different. Therefore, the MCTDHF frequencies must be obtained, and

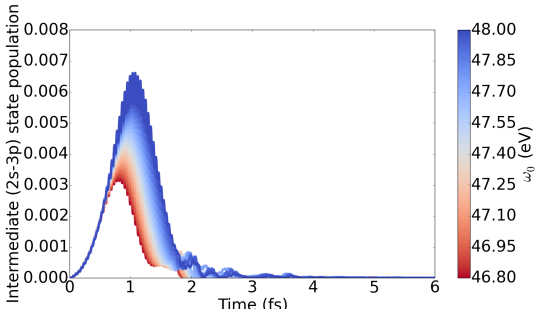

FIG. 2: (Color online) MCTDHF intermediate state (2s-3p) populations for CW pulses at intensities optimized using TDCIS. Pulses are shown for a number of different central frequencies ω_0 (see colorbar) The opening of double and higher ionization channels imposes an intensity limit on the pulses. The optimal intensity at the TDCIS level of theory is above this limit, which leads to ionization rather than populating the intermediate state.

we accomplished this by running various continuous wave (CW) pulses with many central frequencies.

Fig. 2 shows the results of one such set of computations with the peak intensities from the TDCIS optimal pulses. The intermediate state populations are shown, with colors ranging from red to blue for central frequencies from 46.8 to 48.0 eV. The optimal TDCIS intermediate state populations reached around 0.08, but the MCTDHF populations in Fig. 2 are much lower, less than 0.01. At these intensities, the MCTDHF and TDCIS results differ significantly, and the most likely explanation is that multiply ionized pathways are important at these intensities. TDCIS does not take these pathways into account. At an intensity of 6×10^{14} W/cm^2, approximately 3.5 photons/fs cross the atomic radius of Ne, which could lead to the absorption of 2 or more photons and ionize the atom. A reduction of the intensity by a factor of about 4, however, returns the system to the single-excitaton regime which TDCIS can describe.

In Fig. 3, the lower intensity regimes are shown. Intermediate state populations for peak intensities of 10^{14}, 1 and 5 $\cdot 10^{13}$, and $5 \cdot 10^{12}$ W/cm^2 are shown. At these intensities, the intermediate state is populated at the same order of magnitude as estimated by TDCIS at the same intensities. As expected from TDCIS, the higher intensities populate the intermediate state more (as long as the multi-ionization threshold is avoided). At 10^{14} and $5 \cdot 10^{13}$ W/cm^2, intermediate state populations of about 0.02 are reached. This is a factor of 4 lower than the TDCIS result. For both of these intensities, the optimal pump pulse central frequency is found to be 46.8 eV. At the lower intensities, the intermediate state is not populated very much. This is also found at the TDCIS level of theory. As the intensity of the pump pulse is lowered, the optimal central frequency is redshifted.

With the peak intensity and central frequency for the pump pulse fixed at the values determined using the CW pulses, we test the effect of increasing the pulse length

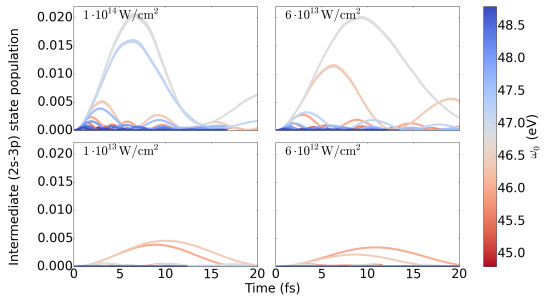

FIG. 3: (Color online) Intermediate state (2s-3p) populations are shown at the MCTDHF level of theory for intensities lower than the optimal TDCIS intensity. The multiple ionization channels are now closed, and the order-of-magnitude of the TDCIS and MCTDHF intermediate state populations are now the same. The optimal central frequency for intermediate state population redshifts as the intensity is lowered. At an intensity of $1 \cdot 10^{14}$ W/cm^2 , the optimal central frequency of the pump pulse is 46.8 eV.

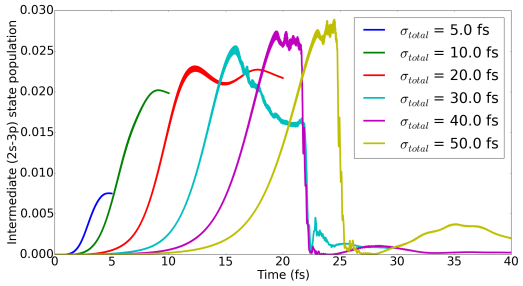

FIG. 4: (Color online) The intermediate state (2s-3p) population is shown for increasing pulse lengths σ_{total}, where the pulse is given by $\mathcal{E}(t) = \mathcal{E}_0 \sin^2(\omega t)$ and $\sigma_{total} = \pi/\omega$. The maximum intermediate state population increases with pulse length, with the increases slowing as the pulse length grows at an intensity of 10^{14} W/cm^2. The TDCIS optimal strategy is to maximize the intermediate state population and then use the Stokes pulse to transfer the intermediate state population to the desired state, and the maximum intermediate state population reachable is around 0.03. Longer pump pulses seem also to induce multiple ionization around the peak of the pulse.

for pulses shaped using a $\sin^2$ function. The results can be seen in Fig. 4. As seen in the TDCIS results (Ref. (LG + KBW)), increasing the pump pulse length is generally favorable. The maximum intermediate state population increases largely at first, and then slightly as the pulse is made longer. An intermediate state population of about 0.03 can be reached using a 50 fs pump pulse, but at these lengths it again appears multiple ionization pathways start to interfere. For the 30, 40, and 50 fs pulse durations a dip in the population can be seen that suggests that higher-order effects are beginning to occur. Since the maximum intermediate state population increases only slightly above 20 fs, and there are no observable multiple ionization effects at this pulse duration, we use the 20 fs pump pulse when determining the optimal Stokes pulse parameters at the MCTDHF level.

Using the same method of determing the optimal central frequency and peak intensity of the Stokes pulse with CW pulses, we determined that the intensity of the Stokes pulse predicted by TDCIS does not introduce multiple ionization pathways. Additionally, a number of calculations were run to determine the optimal central time of the Stokes pulse. The resulting set of pump and Stokes pulses were used to determine the populations of the intermediate 2s-3p and desired 2p-3p states for Raman excitation of Ne, and compared with the optimal TDCIS pulse set in Fig. 5.

Qualitatively, the TDCIS and MCTDHF optimal pulses are very similar. A simple sequential population of the intermediate state followed by population transfer to the desired state can be seen. At the TDCIS level of theory, the intermediate state is populated to a level of 0.08, and about half of this population can be transferred to the desired state. We found in Ref. [13] that coupling between excitation channels induced by electron correlation keeps the entire population of the intermediate state from

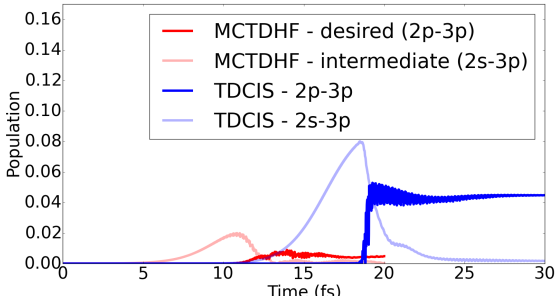

FIG. 5: (Color online) The optimal TDCIS pulse (populations in blue) is compared with a similar (shorter) MCTDHF (populations in red) pulse with the same time ordering. The desired state (dark lines) and intermediate states (light lines) are shown. The qualititative features of the TDCIS and MCTDHF results are the same. The MCTDHF populations are smaller by a factor of about 4.

being transferred to the desired state. At the MCTDHF level of theory, we have already determined that the intermediate state can be populated to a level of 0.02, and this can again be seen in Fig. 5.

IV. CONCLUSION

We have used the multiconfigurational time-dependent Hartree-Fock (MCTDHF) method in order to verify the performance of pulses for x-ray Raman excitation of atoms. This excitation represents the first step towards multidimensional x-ray spectroscopy, a tool for the direct and local measurement of electronic interactions in valence levels. The pulses were obtained us-

ing quantum optimal control theory combined with the time-dependent configuration interaction singles (TDCIS) method. MCTDHF includes multiple excitation pathways that TDCIS does not, and some of these were found to be important. While some care is required to avoid such pathways when using TDCIS, the qualitative features of the processes predicted by TDCIS were found to extend to the more detailed calculations. TDCIS, therefore, is an appropriate tool for optimal control calculations, having the advantages of speed while not sacrificing qualitative accuracy.

Using the combined Krotov optimal control and TDCIS method, we previously determined a mechanism for avoiding ionization while performing the x-ray Raman excitation of atoms. First, the intermediate state is excited using a long pump pulse to selectively address the frequency of the desired transition. Then, a short Stokes pulse is applied near the maximum intermediate state population to drive population to the desired valence state. This pulse sequence avoids ionization, which is mainly due to direct ionization of the spectator orbitals (the 2p orbitals in the case of Ne). This general scheme is supported by the MCTDHF calculations, however some details of its implementation differ from TDCIS. At the intensities that are found to be optimal using TDCIS, multiple ionization pathways are found to occur using MCTDHF. These processes dominate and very little population can be transferred to the intermediate state. At slightly lower intensities, the mechanism found using TDCIS is again qualitatively successful. Quantitatively, a factor of about 4 differentiates the TDCIS and MCTDHF populations. This factor is likely due to competing multiply-excited pathways ignored by TDCIS.

Using TDCIS, we determined that x-ray Raman excitation of Ne was experimentally feasible at the free electron laser facility FERMI@Elettra [27]. The pulses we found to be succesful at the MCTDHF level of theory are also possible at this facility. Specifically, a pump pulse with a duration of 20 fs and power of $0.6\,\mu J$ can be used to Raman excite Ne and avoid ionization.

[1] R. R. Ernst, G. Bodenhausen, A. Wokaun, et al., Principles of nuclear magnetic resonance in one and two dimensions, vol. 14 (Clarendon Press Oxford, 1987).

[2] M. Sattler, J. Schleucher, and C. Griesinger, Progress in Nuclear Magnetic Resonance Spectroscopy **34**, 93 (1999).

[3] V. Kanelis, J. D. Forman-Kay, and L. E. Kay, IUBMB life **52**, 291 (2001).

[4] D. S. Larsen, K. Ohta, Q.-H. Xu, M. Cyrier, and G. R. Fleming, J. Chem. Phys. **114**, 8008 (2001).

[5] M. Khalil, N. Demirdöven, and A. Tokmakoff, The Journal of Physical Chemistry A **107**, 5258 (2003).

[6] S. Mukamel, Annu. Rev. Phys. Chem. **51**, 691 (2000).

[7] D. M. Jonas, Annu. Rev. Phys. Chem. **54**, 425 (2003).

[8] G. S. Engel, T. R. Calhoun, E. L. Read, T.-K. Ahn, T. Manl, Y.-C. Cheng, R. E. Blankenship, and G. R. Fleming, Nature **446**, 782 (2007).

[9] J. D. Biggs, Y. Zhang, D. Healion, and S. Mukamel, J. Chem. Phys. **136**, 174117 (2012), URL http://scitation.aip.org/content/aip/journal/jcp/136/17/10.1063/1.4706899.

[10] S. Mukamel, D. Healion, Y. Zhang, and J. D. Biggs, Annu. Rev. Phys. Chem. **64**, 101 (2013).

[11] S. Tanaka and S. Mukamel, Phys. Rev. Lett. **89**, 043001 (2002).

[12] S. Mukamel, D. Abramavicius, L. Yang, W. Zhuang, I. V. Schweigert, and D. V. Voronine, Acc. Chem. Res. **42**, 553 (2009).

[13] L. Greenman, C. P. Koch, and K. B. Whaley (2014), 1409.7767.

[14] D. Tannor, V. Kazakov, and V. Orlov, in Time-dependent quantum molecular dynamics, edited by J. Broeckhove and L. Lathouwers (Plenum, 1992), pp. 347–360.

[15] J. Somlói, V. A. Kazakovski, and D. J. Tannor, Chem. Phys. **172**, 85 (1993).

[16] A. I. Konnov and V. A. Krotov, Automat. Rem. Contr. **60**, 1427 (1999).

[17] A. Bartana, R. Kosloff, and D. J. Tannor, Chem. Phys. **267**, 195 (2001).

[18] J. P. Palao, R. Kosloff, and C. P. Koch, Phys. Rev. A **77**, 063412 (2008).

[19] D. Reich, M. Ndong, and C. P. Koch, J. Chem. Phys. **136**, 104103 (2012).

[20] L. Greenman, P. J. Ho, S. Pabst, E. Kamarchik, D. A. Mazziotti, and R. Santra, Phys. Rev. A **82**, 023406 (2010).

[21] S. Pabst, L. Greenman, and R. Santra, XCID program package for multichannel ionization dynamics, Rev. 629, with contributions from P. J. Ho. DESY, Hamburg, Germany, 2011.

[22] D. J. Haxton, K. V. Lawler, and C. W. McCurdy, Phys. Rev. A **83**, 063416 (2011), URL http://link.aps.org/doi/10.1103/PhysRevA.83.063416.

[23] D. J. Haxton, K. V. Lawler, and C. W. McCurdy, Phys. Rev. A **86**, 013406 (2012), URL http://link.aps.org/doi/10.1103/PhysRevA.86.013406.

[24] X. Li, C. W. McCurdy, and D. J. Haxton, Phys. Rev. A **89**, 031404 (2014).

[25] D. J. Haxton and C. W. McCurdy, Phys. Rev. A **90**, 053426 (2014), URL http://link.aps.org/doi/10.1103/PhysRevA.90.053426.

[26] K. Bergmann, H. Theuer, and B. W. Shore, Rev. Mod. Phys. **70**, 1003 (1998).

[27] http://www.elettra.trieste.it/FERMI.

[28] J. Caillat, J. Zanghellini, M. Kitzler, O. Koch, W. Kreuzer, and A. Scrinzi, Phys. Rev. A **71**, 012712 (2005), URL http://link.aps.org/doi/10.1103/PhysRevA.71.012712.

[29] O. E. Alon, A. I. Streltsov, and L. S. Cederbaum, J. Chem. Phys. **127**, 154103 (2007), URL http://scitation.aip.org/content/aip/journal/jcp/127/15/10.1063/1.2771159.

[30] M. Nest, R. Padmanaban, and P. Saalfrank, J. Chem. Phys. **126**, 214106 (2007).

[31] M. Nest, F. Remacle, and R. D. Levine, New J. Phys. **10**, 025019 (2008), URL http://stacks.iop.org/1367-2630/10/i=2/a=025019.

[32] T. Kato and H. Kono, Chem. Phys. **366**, 46 (2009), ISSN 0301-0104, attosecond Molecular Dynamics, URL http://www.sciencedirect.com/science/article/pii/S0301010409002869.

[33] D. J. Haxton and C. W. McCurdy, Phys. Rev. A **91**, 012509 (2015), URL http://link.aps.org/doi/10.1103/PhysRevA.91.012509.

[34] A. Goldberg and B. W. Shore, J. Phys. B **11**, 3339 (1978).

[35] R. Santra and L. S. Cederbaum, Phys. Rep. **368**, 1 (2002).

[36] B. Simon, Phys. Lett. A **71**, 211 (1979), ISSN 0375-9601, URL http://www.sciencedirect.com/science/article/pii/0375960179901658.

[37] C. W. McCurdy, M. Baertschy, and T. N. Rescigno, J. Phys. B **37**, R137 (2004), URL http://stacks.iop.org/0953-4075/37/i=17/a=R01.